We ourselves prefer this third explanation. However, more evidence of a quantitative nature is needed to support this suggestion.

We greatly appreciate the stimulating discussions with Dr. H. de Lang and Professor H. G. van Bueren.

[1]H. G. van Bueren, J. Haisma, and H. de Lang, Phys. Letters 2, 340 (1962).

[2]J. Haisma and H. de Lang, Phys. Letters 3, 240 (1963).

[3]H. de Lang and G. Bouwhuis, Phys. Letters 5, 48 (1963).

[4]P. Connes, J. Phys. Radium 19, 262 (1958).

[5]D. R. Herriott, Appl. Opt. 2, 865 (1963).

[6]A. G. Fox and T. Li, Bell System Tech. J. 40, 453 (1961).

[7]A. Szöke and A. Javan, Phys. Rev. Letters 10, 521 (1963).

[8]W. E. Lamb, Jr., Proceedings of the Third International Symposium on Quantum Electronics, Paris, February 1963 (to be published); Proceedings of the Scuola Internazionale di Fisica "Enrico Fermi" on Quantum Electronics and Coherent Light, Varenna, Italy, August 1963 (unpublished).

ANGULAR DEPENDENCE OF MASER-STIMULATED RAMAN RADIATION IN CALCITE*

R. Chiao and B. P. Stoicheff†
Massachusetts Institute of Technology, Cambridge, Massachusetts
(Received 14 February 1964)

One of the most striking characteristics of maser-stimulated Raman scattering is the specific directional emission of the Stokes and anti-Stokes radiation.[1,2] Here, we report on experimental studies of this angular dependence in calcite. We have observed four orders of anti-Stokes emission in well-defined cones, diffuse first-order Stokes emission with cones of absorption in this diffuse radiation, and a well-defined cone of second-order Stokes emission, all in the forward direction. Since the refractive index of calcite is precisely known,[3] it has been possible to predict accurately these maxima and minima of anti-Stokes and Stokes radiation on the basis of the following wave vector relations:

$$\vec{k}_0+\vec{k}_{n-1}=\vec{k}_{-1}+\vec{k}_n, \tag{1}$$

$$\vec{k}_0+\vec{k}_{-1}=\vec{k}_{n-1}+\vec{k}_{-n}, \tag{1'}$$

where $\vec{k}_0$, $\vec{k}_{-1}$, $\vec{k}_n$, and $\vec{k}_{-n}$ are, respectively, the maser, the first Stokes, and the nth-order anti-Stokes and Stokes waves vectors. From these observations it is concluded that in our experiments on the stimulated Raman scattering in calcite, the dominant process is that proposed by Garmire, Pandarese, and Townes.[4]

According to their theory, diffuse first-order Stokes radiation (of frequency $\omega_0-\omega_r$) is initially produced by the very intense maser light (ω_0), and subsequently anti-Stokes and Stokes radiation of many orders ($\omega_0\pm n\omega_r$) is produced by the interaction of the maser light with the first-order Stokes radiation. These higher order Raman effects proceed according to the wave vector relations (1) and (1′) for three-dimensional interactions, and should give rise to absorption of first-order Stokes radiation and to emission of anti-Stokes and higher order Stokes radiation in cones around the maser beam. The theoretical values for the angles of the nth-order anti-Stokes emission from (1) are given by

$$\theta_n=\beta_n\pm(\beta_n^2+\delta_n-\gamma_n)^{1/2}, \tag{2}$$

where

$$\beta_n=k_{n-1}\theta_{n-1}/(k_{-1}+k_n),$$

$$\delta_n=2(k_{-1}/k_n)(k_n+k_{-1}-k_0-k_{n-1})/(k_{-1}+k_n),$$

$$\gamma_n=(k_{n-1}-k_{-1})\beta_n\theta_{n-1}/k_r.$$

The corresponding angles of first-order Stokes absorption are

$$\theta_{-1}^{(n)}=(k_{n-1}\theta_{n-1}-k_n\theta_n)/k_{-1}. \tag{3}$$

Equations (2) and (3) also give the angles of the nth-order Stokes emission and corresponding first-order Stokes absorption when $\vec{k}_n$ is replaced by $-\vec{k}_{-n}$ and $\vec{k}_0$ by $-\vec{k}_0$.

In our experiments, a calcite crystal 5 to 10 cm long was placed in the path of the focused external beam from a giant pulse ruby maser (with rotating prism). The maser output power was in excess of 10 megawatts in a 30-nsec pulse. The crystal was oriented so that the maser beam, which was linearly polarized, traveled through the crystal as the ordinary ray. In this orienta-

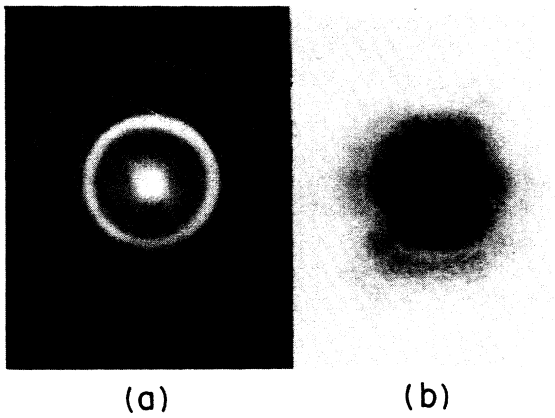

FIG. 1. Stimulated Raman emission from calcite with the vibrational frequency of 1085.6 cm^{-1} excited by the giant pulse ruby maser. (a) Anti-Stokes emission pattern observed with maser beam incident perpendicular to crystal face; (b) Stokes emission pattern (negative image) under same conditions as (a).

tion the vibrational Raman frequency of 1085.6 cm^{-1} was excited,[5] producing several orders of Stokes and anti-Stokes radiation. Photographs of the scattered radiation were obtained on Polaroid type 57 film (ASA speed 3000) placed in the path of the maser beam without the use of a camera lens. Stokes radiation was isolated by placing Corning filters Nos. 2-64 and 7-69 between the crystal and film; anti-Stokes radiation was isolated by using two Corning No. 4-70 filters. Photographs of the second-order Stokes radiation were obtained on Polaroid type 413 infrared film using a Corning No. 5-57 filter to attenuate selectively the first-order Stokes radiation.

Typical photographs of the Stokes and anti-Stokes radiation are shown in Figs. 1 and 2. The intensity maxima in Figs. 1(a) and 2(a) represent the cones of anti-Stokes emission in small angles around the maser beam. The resulting rings are well defined and sharp thus permitting accurate measurement of their diameters. The absorption ring in the diffuse Stokes radiation corresponding to the first-order anti-Stokes emission ring is also clearly demonstrated [Fig. 1(b)], while the outer absorption rings [Fig. 2(b)] are somewhat fainter. By photographing these rings at various distances from the exit face of the crystal (Fig. 3) we were able to determine the point of production of the Raman radiation within the crystal and also the angles of the emission and corresponding absorption. We found that

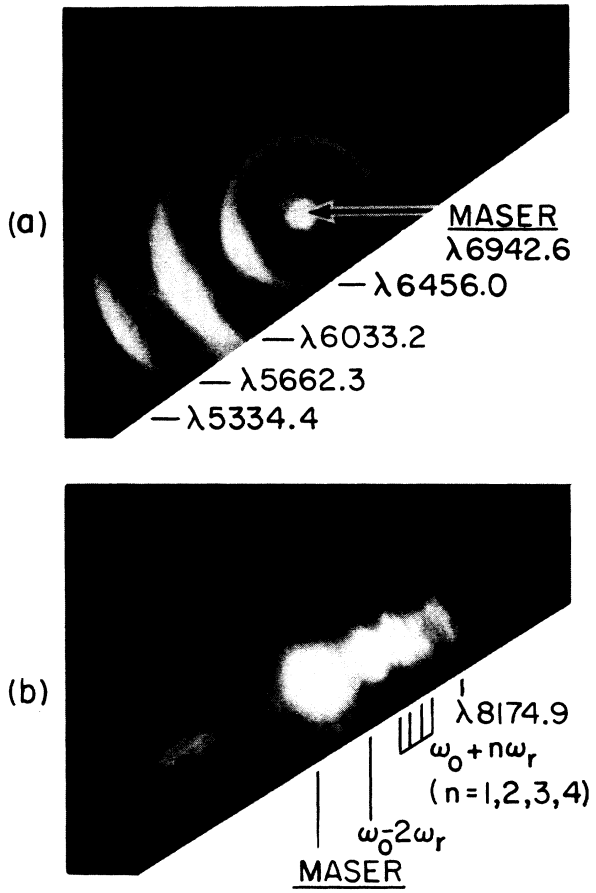

FIG. 2. (a) Anti-Stokes emission pattern from reoriented calcite crystal; (b) Stokes emission pattern (positive image) under same conditions as (a) showing the absorption rings corresponding to $(\omega_0 + n\omega_r)$ and $(\omega_0 - 2\omega_r)$ and also the emission ring $(\omega_0 - 2\omega_r)$ at λ 8174.9.

when the maser beam was focused within the crystal, the Raman radiation was generated at the focal point; when the maser beam was focused after traversing the crystal, the radiation was generated in the region of the exit face. Experimentally, it was found that the emission angles were independent of the crystal used or its length and only slightly affected by temperature (approximately 3% in 100°C). However, there was a significant increase in angle as the focal length of the lens used to focus the maser beam was decreased and as the distance between the crystal and focal point for any lens was decreased. This increase in angle can be explained by the fact that the emission angles are a sensitive function of the magnitude of k_0 which is known to be smaller near the focal point than for a plane wave.[6] We

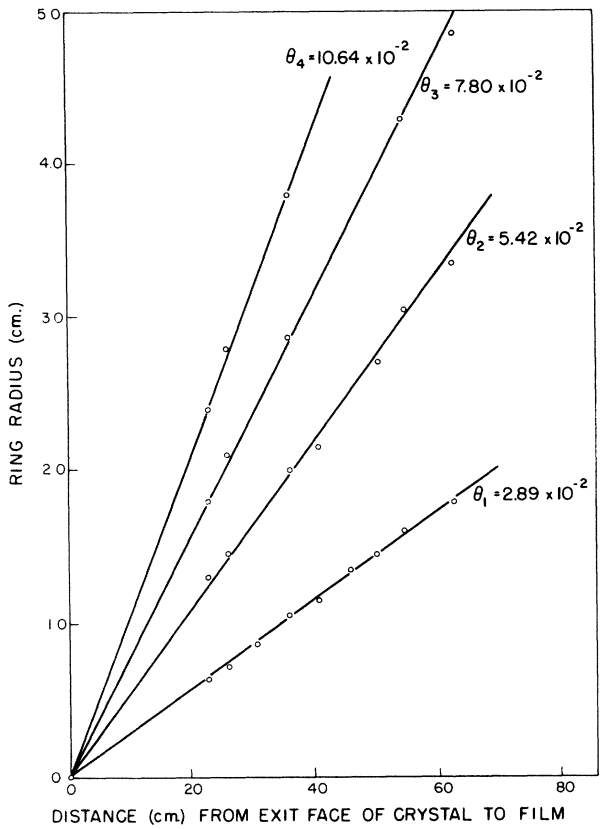

FIG. 3. Determination of emission angle and point of generation of anti-Stokes radiation. Focal length of lens used to focus maser beam on crystal was 30 cm.

therefore extrapolated the angles obtained with lenses of $f = 8$, 20, 30, 50, 127 cm, to the ideal values corresponding to a plane wave ($f = \infty$). These values are listed in Table I.

The calculated values of the angles with the + sign in Eq. (2) were found to agree very well with the experimental values and are given in Table I for comparison. On the other hand, emission (or absorption) rings corresponding to the calculated values with the - sign in Eq. (2) were not observed in these experiments. This result may be explained by the fact that the requisite large-angle ($>6\times10^{-2}$ radian) diffuse Stokes radiation also was not observed in these experiments, evidently because the high gain for stimulated emission is predominantly in small angles around the maser beam.

The symmetrical intensity distribution of both Stokes and anti-Stokes radiation shown in Fig. 1 was obtained when the incident maser beam was perpendicular to the entrance and exit faces of the calcite crystal. With the crystal misaligned by only a few degrees the asymmetrical distribution shown in Fig. 2 was obtained. It is noted that the Stokes and anti-Stokes radiation are on opposite sides of the maser beam, in agreement with the wave vector relation (1). Also, the second-order Stokes emission ring appeared only when accompanied by an intense second-order anti-Stokes emission ring as expected from relations (1) and (1′) (since the same three frequencies are involved in their production); moreover, the second-order Stokes emission and corresponding first-order Stokes absorption appear on the same side of the maser beam [Fig. 2(b)].

Another theory which has been proposed to explain maser-stimulated Raman scattering is that involving four-photon resonant and nonresonant processes requiring the annihilation of two maser photons to produce one Stokes and one anti-Stokes photon. While these processes would also lead to the wave vector relation (1), they predict emis-

Table I. Comparison of the experimental and theoretical values of the emission and absorption angles observed in the maser-stimulated Raman radiation of calcite.

Frequency	Wavelength (Å)	Emission angles (10^{-2} rad) Experiment	Theory	Absorption angles in diffuse Stokes radiation (λ 7508.5 Å) (10^{-2} rad) Experiment	Theory
$\omega_0 - 2\omega_r$	8174.9	5.2 ± 0.1[a]	5.57	1.8 ± 0.1[a]	2.22
$\omega_0 + \omega_r$	6456.0	2.50 ± 0.03[b]	2.49	2.90 ± 0.03[b]	2.90
$\omega_0 + 2\omega_r$	6033.2	5.03 ± 0.08[b]	4.91	3.26 ± 0.06[b]	3.21
$\omega_0 + 3\omega_r$	5662.3	7.64 ± 0.2[b]	7.29	3.50 ± 0.06[b]	3.55
$\omega_0 + 4\omega_r$	5334.4	10.2 ± 0.4[b]	9.61	3.77 ± 0.06[b]	3.86

[a]Obtained with an $f = 20$ cm lens.
[b]Values obtained by extrapolation to $f = \infty$.

sion of both Stokes and anti-Stokes radiation, contrary to our observations with calcite. Further, it was suggested to us by Dr. A. Szöke[7] that since the Stokes radiation has the greatest gain in the forward direction it may be possible to generate cones of anti-Stokes radiation not only as a volume effect according to relation (1) but also as a surface effect according to $\vec{k}_n \cos\theta_n = (n+1)\vec{k}_0 - n\vec{k}_{-1}$. However, for calcite the corresponding values of the angles for the first- and second-order anti-Stokes emission are 3.67×10^{-2} and 6.26×10^{-2} radian, considerably larger than the observed values.

In summary, we note that our experiments with calcite quantitatively confirm the wave vector relations (1) and (1′). In addition, the observed absorption cones in the first-order Stokes radiation show that in calcite the interaction of maser light with the first-order Stokes radiation produces anti-Stokes and Stokes radiation of several orders, in accordance with the theory of Garmire, Pandarese, and Townes.[4]

We are very grateful to Professor C. H. Townes for his interest and advice during the course of this work and to Mrs. E. Garmire and Dr. A. Szöke for helpful discussions.

---

*This work was supported in part by the National Aeronautical and Space Administration under Research Grant No. NsG-330.

†On leave from the National Research Council, Division of Pure Physics, Ottawa, Canada.

[1]R. W. Terhune, Bull. Am. Phys. Soc. 8, 359 (1963); Solid State Design 4, 38 (1963). B. P. Stoicheff, Phys. Letters 7, 186 (1963).

[2]H. J. Zeiger, P. E. Tannenwald, S. Kern, and R. Herendeen, Phys. Rev. Letters 11, 419 (1963).

[3]J. W. Gifford, Proc. Roy. Soc. (London) A70, 329 (1902).

[4]E. Garmire, F. Pandarese, and C. H. Townes, Phys. Rev. Letters 11, 160 (1963); see also reference 2; R. W. Hellwarth (to be published).

[5]G. Eckhart, D. P. Bortfeld, and M. Geller, Appl. Phys. Letters 3, 137 (1963).

[6]M. Born and E. Wolf, Principles of Optics (Pergamon Press, New York, 1959), pp. 434-444.

[7]A. Szöke (private communication).

ENERGY LOSSES AND ELASTIC RESONANCES IN ELECTRON SCATTERING FROM H_2†

C. E. Kuyatt, S. R. Mielczarek, and J. Arol Simpson
National Bureau of Standards, Washington, D. C.
(Received 14 February 1964)

Recently developed techniques of high-resolution electron spectroscopy[1] have both given new information on the energy levels of rare gas atoms[2] and made possible the discovery of sharp resonances in the elastic scattering of electrons from rare gases.[3,4] These techniques have now been used to study the simplest and theoretically best-understood molecule, hydrogen. Inelastic scattering measurements for the first time show well-resolved vibrational levels of several electronic states of H_2. Elastic scattering measurements show at least eight narrow resonances in the elastic cross section.

The experimental apparatus, previously described,[5] consists of an electron energy monochromator, a gas-filled scattering chamber, and an electron energy analyzer. The analyzer accepts only electrons which are within a cone of half-angle 0.0125 rad about the direction of the incident electron beam. In the elastic measurements only electrons which have lost less than about 0.05 eV are accepted.

Figure 1 shows the variation of the number of 33-eV electrons inelastically scattered by 0.04 Torr-cm of hydrogen as a function of electron energy loss. Two vibrational series are clearly shown, one starting at 11.19 eV and the other at 12.27 eV. The region above 14 eV appears to be composed of at least two overlapping series.

Also shown on Fig. 1 are the rotational bandheads of some of the energy levels obtained from ultraviolet emission spectroscopy by Hopfield,[6] Herzberg and Howe,[7] and Monfils.[8] The ultraviolet data show that the electron energy-loss spectrum arises from excitation of the ground (X) state of molecular hydrogen, $(1s\sigma)^2\,{}^1\Sigma_g^+$, to vibrational levels of three electronic excited states: $1s\sigma 2p\sigma\,{}^1\Sigma_u^+$, $1s\sigma 2p\pi\,{}^1\Pi_u$, and $1s\sigma 3p\pi\,{}^1\Pi_u$, the so-called B, C, and D states.[9] The $1s\sigma 2s\sigma$-${}^3\Sigma_g$ repulsive state, found by Schulz[10] with the trapped-electron method, could not be seen in our measurements. We conclude from our measurements that the probability of exciting this state in forward scattering must be less than 10^{-3} of

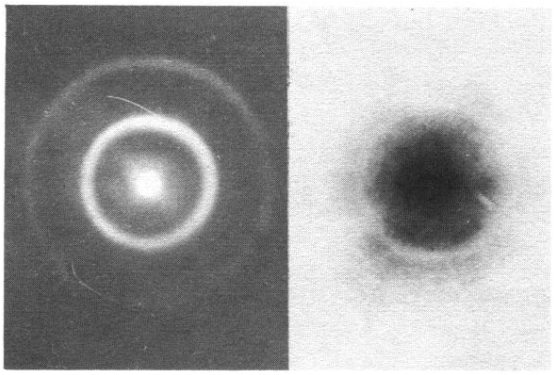

FIG. 1. Stimulated Raman emission from calcite with the vibrational frequency of 1085.6 cm^{-1} excited by the giant pulse ruby maser. (a) Anti-Stokes emission pattern observed with maser beam incident perpendicular to crystal face; (b) Stokes emission pattern (negative image) under same conditions as (a).

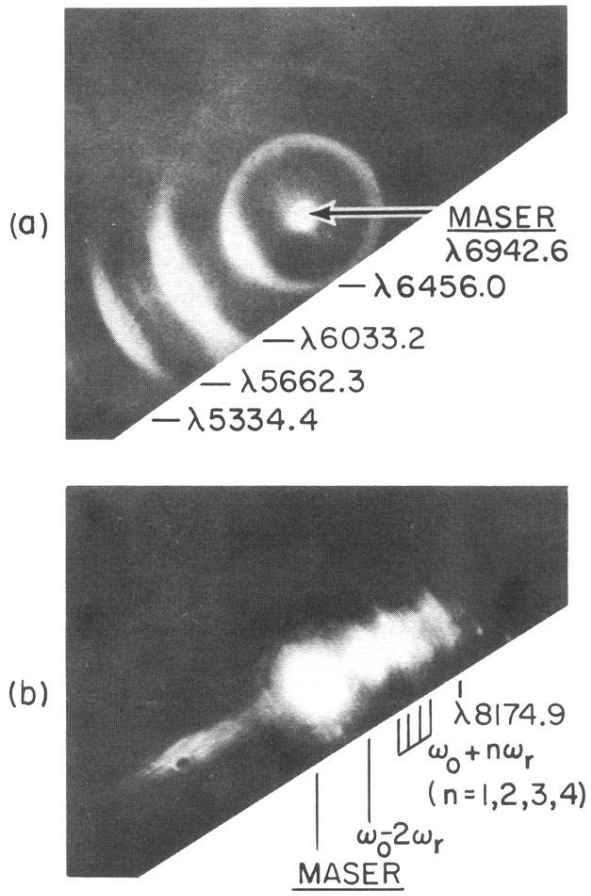

FIG. 2. (a) Anti-Stokes emission pattern from re-oriented calcite crystal; (b) Stokes emission pattern (positive image) under same conditions as (a) showing the absorption rings corresponding to $(\omega_0 + n\omega_r)$ and $(\omega_0 - 2\omega_r)$ and also the emission ring $(\omega_0 - 2\omega_r)$ at λ 8174.9.